RESEARCH ARTICLE

Design and Testing of a Composite Pressure Hull for Deep Autonomous Underwater Vehicles

MOUSTAFA ELKOLALI AND ALEX ALCOCER

OsloMet Oceanlab, Department of Mechanical, Electronic and Chemical Engineering, Oslo Metropolitan University, 0130 Oslo, Norway

Corresponding author: Moustafa Elkolali (elkolali@oslomet.no)

ABSTRACT This paper outlines the design and testing process of the hull of a deep small Autonomous Underwater Vehicle (AUV), rated at 2000m depth. Many existing AUV pressure housings use aluminum or other isotropic traditional metals, instead of composites due to the complexities of the design of composites at such big load. The research at hand explains the process of design starting from setting the geometrical constraints for the design to mass production. To the best of the authors' knowledge, none of the previous studies has presented such detailed description of the work. Carbon fiber reinforced epoxy material was chosen thanks to its high strength-to-weight ratio and similarity of its compressibility to sea water. Material characterization was performed to obtain the material properties under loading conditions using a modified method of the Combined Loading Compression testing technique. A specific fixture was designed and manufactured to test filament-wound tubes. An analytical model was developed using MATLAB, a finite element model was created using ABAQUS, and the results of the two models were compared. A set of recommendations was introduced for the stacking sequence to provide the lowest possible stresses, regardless on the diving depth of the vehicle. Afterwards, a quality control set of tests was conducted, including seawater absorption under high pressure and void analysis using destructive and non-destructive tests. Pilot samples were manufactured and tested in a pressure vessel, where it was cycle-tested and inspected using visual and ultrasonic testing. Other samples were fail-tested and showed a failure at ∼93% of the expected failure load. Such range can be considered good to provide safe operation for the vehicle at the designated depth, given that the factor of safety included covers more than 7% of the failure load. The proposed design methodology has shown that CFRE can be safely used even at such high depths.

INDEX TERMS Composite materials, design for manufacture, finite element analysis, marine vehicles, materials testing, underwater structures.

I. BACKGROUND

The hull of an Autonomous Underwater Vehicle (AUV) is one of the most significant components determining the total compressibility and drag of the vehicle. Since these parameters have a substantial influence on the vehicle's durability and cost; a smart hull design shall be critical to its performance. The main role of the hull is to provide sealing for the electronics, batteries, and other pressure intolerant components as well as having a low drag and low compressibility.

The associate editor coordinating the review of this manuscript and approving it for publication was Haiyong Zheng.

Some vehicles have a single hull that fulfills both tasks, while others have their hull divided into two parts, pressure housing, and flooded fairings that reduce the drag of the vehicle. This fairing that may cover the entire pressure housing it might consist of smaller parts that are attached to the housing at the bow and the stern of the vehicle. These flooded fairings are pressure-tolerant, and they provide better drag properties, especially for the sensors that are subject to seawater. These sensors, even when optimized, can count for up to 35% of the total drag of the vehicle [1].

The other main characteristic is the compressibility of the hull. Barker [2] divided the types of hulls into two types,

compensating and non-compensating hulls. Diving into high depth, the outside pressure increases, while the inside pressure does not. The hull experiences compression stresses, which results in a reduction in its overall size. Bearing in mind that the mass of the vehicle does not change in such operation; the vehicle requires more force to surface, which results in higher energy consumption. The compressibility of the compensating hull equals the compressibility of seawater; hence, lower energy is used since it is not required to use extra buoyant force, unlike the non-compensating hulls. A typical hull that has low compressibility of a standard size AUV loses about 0.1kg of buoyancy during the dive from the surface to a depth of 1000m [3].

"ecoSUBμ5'' vehicle is one of the ecoSUB family of AUVs that are characterized by having a small size; low weight, and low cost. They are ideally suited to be used as nodes in a network and to be deployed in a fleet [4]. According to Fenucci *et al.* [4] and Phillips *et al.* [5], ecoSUBμ5 has a central cylindrical pressure housing that contains the electronics and batteries, attached to two flooded fairings for the nose and the tail of the vehicle, to increase the hydrodynamic efficiency. The pressure housing is made from aluminum that sustains compressive stress up to 1000m depth. The pressure housing contributes to about 33% of the total mass of the vehicle [5]. Another AUV studied is the "HUGIN 1000''. Hagen *et al.* [6] depicts the development process of HUGIN 1000 and how it was derived from the "HUGIN 3000'' AUV which was considered too big for some applications. The HUGIN 1000 was designed for high flexibility to make it fit for different types of missions and applications in both military and civilian domains. According to Hagen *et al.* [6]; the hull of the vehicle has four main advantages. It has high hydrodynamic efficiency, high maneuverability, high hydrodynamic stability, and low acoustic noise [7]. The hull has three sections, with a center section that can have different internal structures, depending on the application to ease its accessibility and maintenance as well as allow different payloads. The hull of "HUGIN 1000'' is made of carbon fiber laminates and high-performance syntactic foam and the pressure containers for the payload and the control are made from seawater resistant aluminum [7].

With regard to for underwater gliders, which are a special type of AUVs that relies on buoyancy to develop their motion, Seaglider vehicle has a compound hull. A drag-efficient fairing hull, that encloses the pressure housing inside. According to Davis *et al.* [3], Eriksen *et al* [8], and Wood [9], the fairing is made of fiberglass-reinforced polyester resin manufactured by filament winding. The fairing supports the wings of the glider, the vertical stabilizer, and the antenna. The axisymmetric low drag shape of Seaglider can maintain laminar flow over more than 80% of its surface even at high speeds that can reach 7m/sec [8]. Gliders, never operate at such high speeds since in general, they are slow in their nature compared to AUVs, which makes them even more susceptible to biofouling [10]. It is worth mentioning that Seaglider had a conductivity sensor on its nose that had only

2% of the cross-sectional area of the glider's nose. However, this sensor was counted for more than 25% of the total drag of the vehicle, which confirms the statement already mentioned earlier about how important placing the wet payload and sensors on the glider is. The pressure housing of Seaglider consists of several deflecting arched panels made up of aluminum, which is supported by ring supports, to have similar compressibility as the seawater. The vehicle loses only about 0.5g of buoyancy force over a pressure change of 500m [8]. The pressure housing consists of 7 different sections, two in the front joint permanently, and the rest can be dismantled to ease maintenance.

During their lifetime, underwater gliders perform many cycles under different depths, which means different loading conditions. This means that the hull of the vehicle experience not only static loads but also might experience fatigue. Changli *et al.* [11] studied the effect of deep cycles on the fatigue life of a deep, 7000m class, submersible pressure hull.

This paper introduces the steps of designing an underwater hull made of composite material and all the processes, shown in Fig. 1, that it goes through, starting from specifying the dimensions and shape of the hull, up to mass production. Figure 2 shows the five steps of the design which are going to be further explained in the following sections.

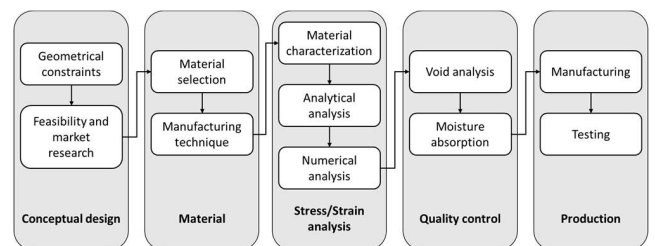**FIGURE 1.** An assembly of the underwater vehicle, showing the designed pressure hull in yellow and the fairings in black.

FIGURE 2. Steps of design and manufacturing of a composite product.

II. METHODOLOGY

A. CONCEPTUAL DESIGN

The first step of the design is to define the dimensions of the hull based on the components onboard, such as sensors, electronics, batteries, etc. This step, although might seem obvious, will define the stresses acting on the hull and hence, define every other step in the design process.

The second step in a conceptual design is a feasibility study and market research on the potential materials and their manufacturing techniques based on the geometrical constraints required. The choice was made to use composites. The main

rationale for using composites is that, in general, they have higher strength-to-weight ratios than isotropic materials, such as metals [12]. For instance, it is less efficient to build the hull, which is a pressure vessel, out of isotropic materials because the stresses in the longitudinal direction only use half the load-carrying capacity of the structure, unlike in composites where the angles of the laminas can be optimized to have thinner wall thicknesses, resulting in a lighter structure.

According to Osse and Lee [13], in 1989 a research project attempted to manufacture high-pressure hulls with an outside diameter of 20cm. The project cooperated with five companies to manufacture a total of 23 hulls using both filament winding and hand layup of 6 types of fibers and 9 types of resins and all 23 of the prototypes produced prematurely. Many manufacturing faults were reported, but the most common among them were fibers wrinkling, and voids [14]. They also made fatal mistakes in the design such as assuming that the composite has similar compressive and tensile strengths, as well as treating each layer as an isotropic one, by performing only uniaxial testing to obtain the strength of the material [13]. Byon *et al.* [15] reported that even in hydrostatic compressive loads, some of the inner laminae might experience tensile stresses in the radial direction. These radial stresses might lead to delamination failure, if not counted for. This was one of the main points taken into consideration during the design, by choosing the optimum stacking sequence and simulating the behavior of the matrix layers between the lamina to avoid delamination. This discussed in more detail later.

Osse and Lee [13] developed an autonomous underwater vehicle hull that is capable of diving to a depth of 6000m from Carbon/Epoxy composite, by using filament winding. They tried three composite materials, made up of from a combination of two fiber types and three epoxy resins (T700/G94, T700/UF3352, and IM7/8552). They manufactured the cylinders and carried out both characterization and quality control tests in collaboration with three different companies, Boeing Co. Phantom Works Division, ATK Composites (acquired by Northrop Grumman), and HyPerComp Engineering. However, they committed two mistakes during testing, which made the results unrealistic. The first one was that the characterization test coupons were made using the ''hot plate press'' curing technique, rather than ''autoclave''. The testing, in this case, does not count for any manufacturing flaws, whether they are resulting from autoclave curing. In other words, the compressive and tensile conducted performed on the rectangular coupons did not capture the real conditions. The second mistake is that they performed matrix ignition tests on filament-wound ring samples to calculate the fiber/matrix volume fraction and to include corrected properties of the material based on the actual volume fraction in their design. The fiber volume ratio was around 55%, however, they did not calculate the voids percentage from these tests and although one of the three companies performed acid digestion tests on their samples, they did not include a voids-correction factor for the material properties.

Two manufacturing methods can be used to manufacture the cylindrical and semi-cylindrical pressure hulls made up of composites, filament winding, and sheet wrapping. Both methods can be used for manufacturing hollow symmetrical components, by using a rotating mandrel. The use of mandrel ensures uniformity in the inside dimensions of the final product [16]. In sheet wrapping, also known as roll wrapping, a pre-impregnated sheet, either unidirectional or ±45°, is cut based on the required angle and press-wrapped around a mandrel forming a single lamina. The process is simple, it does not require special treatment, and the surface finish is higher than the filament winding technique. Another paramount advantage of this technique is that the fibers can be stacked precisely at 0° and 90°, which results in a better hoop and longitudinal strength for the manufactured component. The process also does not have crossed fibers if unidirectional sheets are used, which reduces the cavities and the voids that can result from manufacturing. It also allows the wrapping of different composite materials during stacking, allowing hybrid designs more conveniently. However, the process is less automated, necessitating the use of skilled labor, which in return causes the manufacturing expenses to be higher, and the process is less common than filament winding. Filament winding, on the other hand, is highly automated, numerically controlled, and optimized. Hence, the production is faster and carried out in one cycle, which makes it ideal for mass production. Although the production process is fast, compared to roll wrapping, the preparation time is long, so it is not practical to use this technique to produce a single unit. The technique might produce pores more easily due to the entanglement of the fibers at different layers, which necessitates post-manufacturing quality control inspections, either by using destructive or non-destructive testing. The filament winding technique was selected for manufacturing based on the performed market research, availability, price, and lead time.

During a filament winding process, a significant number of fibers are drawn from creels, commercially known as bobbins, into a bath with liquid resin (above its glass temperature), curing agent, catalyst, and other possible chemicals, such as pigments. Fiber guides control the fibers' tension between each creel and the resin bath. The fibers are then drawn through a wiper at the end of the resin bath to remove any excess resin and regulate the coating thickness surrounding each fiber band. The most common wiper device is a series of squeeze rollers that control both the matrix content and the tension in the fiber band by adjusting the position of the top roller [16]. Finally, the flat band of fibers is then positioned on the rotating mandrel by a moving carriage that moves in parallel to the axis of the mandrel, creating different layers of the material. The crucial process parameters in a filament winding operation are fiber tension, fiber wet-out, and resin content. Adequate fiber tension is essential to maintain fiber alignment on the mandrel as well as to control the resin content in the wound part. Excessive fiber tension might cause discrepancies in resin content in the inner and outer

layers, undesirable residual stresses in the finished product, and large mandrel deflections.

Fiber tension and fiber wet-out, are essential process factors in a filament winding operation. adequate tension is required to control the fiber alignment and the resin content. Over-pulling the fibers might result in a different resin content between the layers and unwanted residual stresses in the final product [17]. Fiber wet-out, however, is fundamental to reduce the voids in the final part. The fiber wet-out during filament winding depends mainly on the viscosity of the matrix, which is subject to the percentage of the hardener and the temperature of the bath. It also depends on the tension and the speed at which the fiber band is being wound in, around the layers that are already wound around the mandrel [17]. This causes the matrix in the wound layers to be squeezed out, which results in voids and different fiber/matrix volumetric ratios in these layers. The most common flaws that might result from the filament winding process are voids, delamination, and fiber wrinkling. Voids act as stress intensifiers and facilitate crack propagation which reduces the mechanical properties of the material and may result in a premature failure. Delamination occurs if the time period between winding each layer is big, particularly if the part being manufactured is large or if the resin has a low pot-life. In this case, adding an extra layer of matrix on the wound layer, by using a brush, for example, is recommended before winding the new one. Wrinkles result from incorrect winding tension or from winding on insecure pathways on the mandrel, resulting in fibers slippage, bridging, and misorientation of the fibers.

B. MATERIAL SELECTION

The choice of the material is the principal parameter for the design of a composite structure. Usually, this process starts by selecting the fiber [16]. The choice of metals and other isotropic materials was excluded, as explained earlier, rather than composites and after choosing the manufacturing technology based on the market and feasibility study carried out, the potential materials were narrowed down into two alternatives, Carbon/Epoxy, and Glass/Epoxy composites. Using Kevlar fibers or Ceramics was unreasonable and overpriced for the application, given the applied loads and the surrounding environment. Carbon fibers are approximately 20-30% lighter than glass fibers' and their longitudinal modulus of elasticity is roughly 3 times of glass fibers [18]. The specific strength of the standard modulus carbon fibers is 1.65 times the E-glass and 1.3 times the S-glass [12], which makes them more favorable since the structure will be lighter. The material chosen for manufacturing is Torray®T-700 Standard Modulus carbon fibers, with epoxy Hexion®EPIKOTE 828 as a resin mixed with EPIKURE 866 curing agent and EPIKURE 101 catalyst with the ratio of 100:80:1.5 by weight, respectively.

Two main issues were faced during the literature review of the material to know its mechanical properties. The first one is that although the composite chosen is very popular and used widely in many industrial and research applications, a wide range of the values of the mechanical properties was found with huge differences in comparison to the datasheets and other research work. The second problem is that some of the parameters do not exist neither in datasheets nor in scientific articles. Most of the parameters stated are in tension, while most of the compression values were missing. Table 1 shows a comparison between "Toray" T-300 composite and fiber properties from different resources. It is obvious that not only does a wide variation exist between the values of the properties, but also many properties are missing (the shaded cells) which are important to the design. These values, even if assumed, will result in completely wrong predictions of the stresses and the strains in the laminas, which led to the necessity of the experimental tests performed and explained in the following section.

The missing values from the fiber properties prevented the possibility of using the rule of mixtures to estimate the missing composite properties. Although the error of the rule of mixtures might be big and could reach 40% in some cases [17], it is useful to provide a rough prediction of the properties of the composite, on the basis of the ones of the fibers and matrix. It also eliminates the possibility of assuming that the load is carried entirely by the fibers, which even though this assumption is conservative, would be helpful in a preliminary design.

C. STRESS/STRAIN ANALYSIS

The problem brought up in the previous section dictated that the chosen composite has to be characterized by testing to get the properties of the material, especially the compressive properties. It is an essential step for the next phases of the design.

1) MATERIAL CHARACTERIZATION

Standards [19], [20], [21] describe the characterization of polymer matrix composite materials, in tensile and compressive loading. The problem is that such standards are designated for the rectangular cross-sectional area samples. The chosen manufacturing technique, filament winding, might only produce hollow axis-symmetric samples. One solution is testing samples that are wound on a flat mandrel and cured by the "hot press" technique. Although the material used will be the same, the results will not be entirely correct, since manufacturing using a hot press produces different void content, as stated earlier. Henry *et al.* [22] introduced a method of testing the material, by compressing filament-wound tubes. Compressing the entire tube will result in crushing the edges of the two ends of the material. In order to avoid this complication, they inserted steel endcaps in the two ends of the tubes and potted them using a bismuth alloy. This solution, although proven to be feasible, is complicated and expensive. A total of 12 samples were to be tested in compressive loading only. This means that 24 endcaps were to be manufactured, press-fitted in the tubes, and potted using a low-melting temperature alloy, which was not practical. Instead, the wound tubes were sliced longitudinally into four pieces, as shown in Fig. 3. This

TABLE 1. Properties of Standard Modulus Uni-directional Carbon/Epoxy composite.

Property	Unit	Loading	Composite properties, (60% fiber volume)		Fiber properties		
			Reference [18]	Material datasheet	Reference [23]	Reference [24]	Material datasheet
strength in the longitudinal direction σ_{11}	MPa	Tension	1270	1860	3530	3500	3530
		Compression	1130	1470	1800	1800	
strength in the transverse direction σ_{22}	MPa	Tension	42	76			
		Compression	141				
In-plane shear strength τ_{12}	MPa	Shear	63	98			
Interlaminar shear strength τ_{23}	MPa	Shear	90	107			
modulus in the longitudinal direction E_{11}	GPa	Tension	134	135	230	210	230
		Compression			106	106	
modulus in the transverse direction E_{22}	GPa	Tension	7				
		Compression					
In- plane shear modulus G_{12}	GPa	Shear	4.2		14		
Major Poisson's Ratio υ_{12}			0.25				
Maximum strain in the longitudinal direction ε_{11}	%	Tension		1.3		1.68	1.5
		Compression					
Maximum strain in the transverse direction ε_{22}	%	Tension					
		Compression					
Maximum in-plane shear strain ε_{12}	%	Shear					

eliminated the need to manufacture many cylinders or to use endcaps. To overcome the problem of clamping the samples between the grips, a special testing fixture was designed and manufactured, as shown in Fig. 3. The fixture had two main parts one is male to clamp on the inner side of the tube, and one is female to clamp on the outer side of the tube. For ease of manufacturing, the fixtures were made up of stainless-steel sheets that are assembled together to give the required shape. The testing machine used is "Shimadzu-AG100kNNXplus".

Three groups of four samples each were tested using combined loading compression [20], [25]. The specimens' dimensions and ply orientation are demonstrated in Table 2. The dimensions was chosen to follow the recommendation of standard [20].

A group of samples was wound at the maximum winding degree to test the transverse properties and another group is wound at ±45° to get the in-plane shear properties following the methodology of [26]. However, winding tubes at angles ±6° only, the minimum winding angle, is not unpracticable in manufacturing, especially for such a small thickness (2.6mm), since the axial force resulting from the extractor that removes the mandrel might damage the manufactured tube. The damage induced has a high possibility of being invisible, such as delamination, which will give false findings during the test analysis. Two hoop layers were added to prevent such damage, and the longitudinal properties were back-calculated given the knowledge of the transverse and in-plane properties using classical lamination theory. A technique that is previously used by Henry et al.[22] as well as Adams and Welsh [25] in their work.

The area of each sample can be geometrically calculated, by using a Computer Aided Drafting (CAD) software, or by using the methodology of standard [27] to calculate the volume of the sample, by measuring the weight of the sample before and after submersion in distilled water at a given temperature. The variance between the two measurements represents the buoyancy, that can be used to calculate sample volume. Given that the length can be measured easily, using a caliper or a micrometer, the area can be calculated from the volume measured.

The test method proved practical and efficient in the first and the second group, as shown in Table 3. However, the method was not effective with the third group, which had the stacking sequence of $[6°_2 87°_1]_S$. Many of the samples failed prematurely and failed at unacceptable areas, outside the gage length, as shown in Fig. 4. Fifty percent of the samples were rejected, and only 2 samples showed acceptable results.

Only the modulus can be back-calculated from this set of tests, and the modulus was around 17% less than the value stated in the datasheet. The unacceptable failure could have occurred due to several possible reasons. A slight deformation in the testing fixture could have been the reason for such anomaly, because the two samples that revealed the unexpected failures were the last to test. Another reason is that the two samples might not have been fixed properly, or any other flawed testing procedure could have occurred.

The properties of the tested composite are summarized in Table 4.

TABLE 2. Properties of the 12 tested specimens and the measured property in each.

Group	Number of samples	Stacking sequence	Mandrel diameter (mm)	Outside diameter (mm)	Specimen length (mm)	Gage length (mm)	Tab length (mm)	Property measured
1	4	$[45°]_7$	36	41.32	140	12	64	In-plane shear
2	4	$[87°]_{13}$	36	40.16	140	12	64	Transverse
3	4	$[6°_2\ 87°_1]_S$	28	33.28	140	12	64	Longitudinal
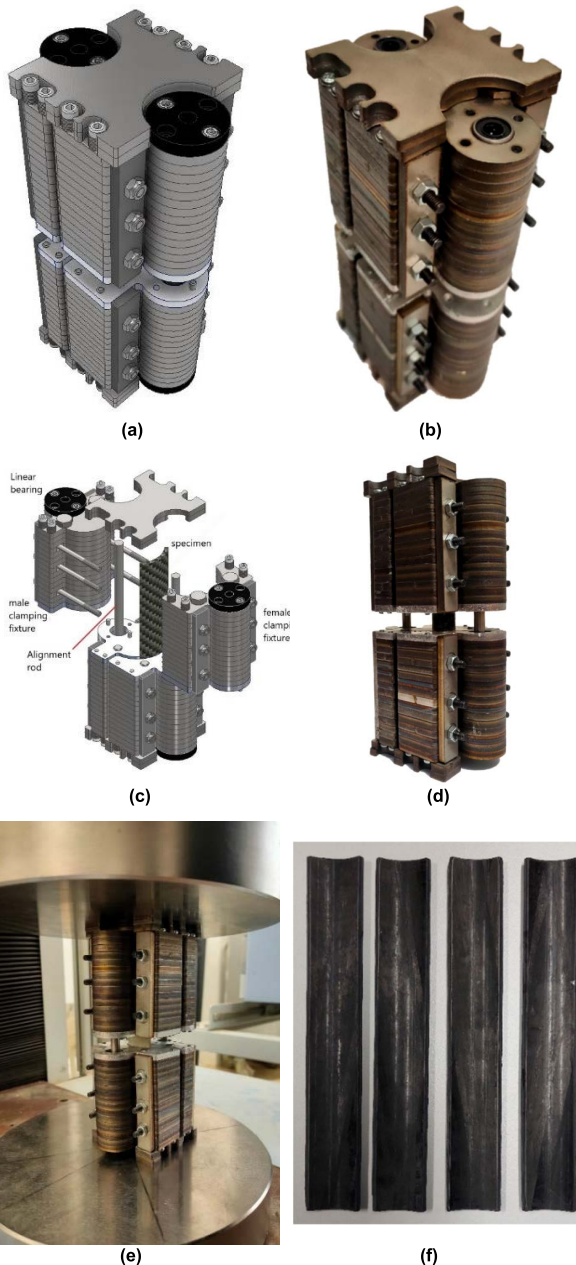
FIGURE 3. Material characterization and testing features; (a) 3D CAD model of the designed fixture; (b) The assembly of the manufactured fixture; (c) Exploded view of the assembly; (d) The specimen being fixed in the fixture; (e) the assembly under loading in the testing machine; (f) the tested specimen's shape.

2) ANALYTICAL ANALYSIS

The working pressure of the pressure vessel can be increased, or the wall thickness might be reduced by choosing the most appropriate winding angles for the laminate.

Messager *et al.* [28] performed an optimization on the lamination angles for thin underwater composite hulls by employing genetic algorithms. The results were validated using both a Finite Element Model (FEM) and experimental testing using Carbon/Epoxy and Glass-Epoxy composite cylinders. They concluded that the optimal lamination would have the following pattern $[\theta_{N1}/\varphi_1/\lambda_{N2}/\varphi_2/\theta_{N3}]$, where θ is the maximum winding angle ($\sim$90°), λ is the minimum winding angle ($\sim$0°), and φ is a transition zone angles. Some previous literature used approximations, numerical and analytical methods to conclude that for filament winding of pipes, the optimum angle if both axial and radial stresses are considered is 55°, such as [29], [30], [31], while others came to the same results experimentally by testing several wound tubes with different angles under different loading conditions, such as Hamed *et al.* [32]. These results are also well-known in the industry.

Using the different conclusions of previous literature, the following recommendations were considered while determining the stacking sequence;

1. The stacking sequence has to be symmetrical, to eliminate the Shear-Extension, Bending-Extension, and Bend-Twist couplings from the "ABD" matrix, reducing the stresses acting on the different plies of the hull.
2. Three angles are used in the stacking sequence, a minimum winding angle that carries the axial stresses, a maximum winding angle that carries the hoop stresses, and a transitional angle between them. The hoop stresses are twice the longitudinal ones, hence the angles should follow the same rule.
3. The plies of each angle are grouped to reduce the interlaminar shear stresses (ILSS) between the different plies.
4. The transitional angle is 55° since it is the optimum angle.
5. Finally, the hoop layers ($\sim$90°) should be on the top and the axial layers ($\sim$0°) should be in the middle.

The resulting stacking sequence from these recommendations should be $[\theta_{2x}/55°_y/\lambda_x]_S$, where θ and λ are the maximum and minimum possible angles that the winding machine can produce.

A model was created on MATLAB software to calculate the ABD matrix and resulting stresses and strains in each layer. This model represents a simple way of modeling the problem with less time and computational resources than the numerical simulation. It is also a helpful tool to monitor the resulting stresses of adding, removing, changing the angles, or changing the sequence of different layers' stresses.

TABLE 3. Results of the 1st and 2nd group of specimens.

Laminate	Specimen	Modulus E_{xx} (GPa)	Max. Strength σ_{xx} (MPa)	Max. Strain ε_{xx} (%)	Laminate	Specimen	Modulus E_{xx} (GPa)	Max. Strength σ_{xx} (MPa)	Max. Strain ε_{xx} (%)
$[45°]_7$	1	18.22	232.18	5.62	$[87°]_{13}$	1	13.51	240.13	2.33
	2	18.90	222.61	3.69		2	13.49	240.41	2.03
	3	18.07	222.67	3.69		3	14.33	256.30	2.45
	4	19.07	246.25	4.55		4	10.98	229.86	2.54
	Avg.	18.56	230.93	4.39		Avg.	13.08	241.67	2.33
	St. dev.	0.493	11.163	0.92		St. dev.	1.452	10.915	0.22
	CoV (%)	2.66	4.834	20.89		CoV (%)	11.10	4.51	9.51

(a)

(b)

FIGURE 4. Failure in the tested specimens; (a) accepted failure areas within the gauge length, (b) unacceptable failure areas.

TABLE 4. Properties used in the design.

Property		Unit	Direction	Value Measured	Value Data sheet
Compression strength	σ_{11} σ_{22}	MPa	Longitudinal Transverse	- 241.67	1470 -
Modulus	E_{11} E_{22}	GPa	Longitudinal Transverse	112.5 13.08	135 -
In-plane shear strength	τ_{12}	MPa	Shear	61.78	98
In-plane shear modulus	G_{12}	GPa	Shear	5.028	-
Maximum strain	ε_{11} ε_{22} ε_{12}	%	Longitudinal Transverse Shear	- 2.33 1.66	- - -

with each layer only half of its thickness, treating each lamina as a balanced plain weave [18]. A step that is not entirely necessary but provides more accurate results of the stresses.

3) NUMERICAL SIMULATION

The numerical simulation was executed using ABAQUS software [34]. This step is vital to study and analyze the stresses in the parts of the hull that cannot be studied analytically., such as the interface between the composite hull and the metal endcap, at the end of each side. Such an interface, between two different materials with different moduli of elasticity, can produce extra stresses that might damage the laminate.

The major in-plane stresses and strains of each lamina are studied and compared to the MATLAB model. The results of the two models, which are shown in Fig. 6, matched each other which validates both of them. Regarding the effect of the endcap, the stresses and strains of each layer across the length are also displayed in Fig. 7. Only the first and last ply in each ply group are visualized in Fig. 7. Although the loads applied on the hull are purely compressive, it was clear that some layers are experiencing tensile stresses due to the endcap, confirming the findings of Osse and Lee [13], and Byon et al. [15].

Although none of the stresses or the strains passed the critical limit, there are important stresses that are not modeled yet, which is the out-of-plane stress of each layer, or the
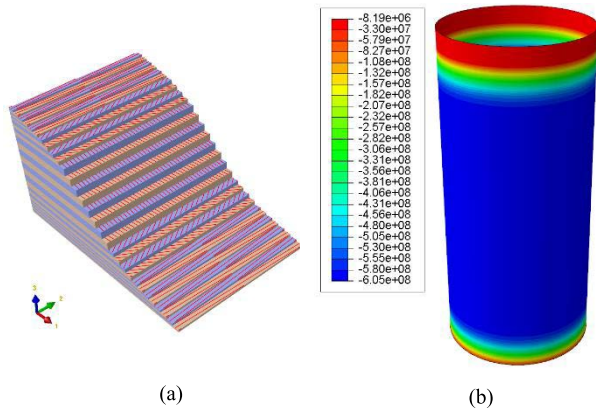
The analytical model can also be used as an efficient tool to calculate the thermal stresses and hygral stresses if there are any, faster and much simpler than the numerical simulation. The resulting forces could be inserted into the numerical simulation, as external forces, rather than calculating them in the model.

The stacking sequence used is $[87°_4 / 55°_2 / 6°_2]_S$. It appeared that switching the position of the 6° layers and the 87° layers, produced higher stresses, confirming the results of the genetic algorithms of Messager et al. [28] and Almeida et al. [33]. However, the difference was not significant, only in the range of "kPa". The results from the MATLAB model were used to validate the numerical model that is explained in the following section.

However, winding at angles such as 55° and 6° is not physically possible in filament winding machines. Instead, the winding of each layer is actually $\pm\delta°$. Hence, the actual stacking used in the MATLAB model, as well as the numerical simulation, is $[(87°/-87°)_4 / (55°/-55°)_2 / (6°/-6°)_2]_S$,

(a)   (b)

FIGURE 5. Model created in ABAQUS; (a) visualization of the stacking sequence, (b) visualization of the stress in one of the layers.

(a)

(b)

FIGURE 6. A comparison between the "through-the-thickness" results from the analytical model and the FE model, without taking the endcap into count, where the MATLAB results are marked as "ML" and the ABAQUS results are marked as "AQ"; (a) the in-plane stress components, (b) the in-plane strain components.

ILSS. There are two methods of modeling these stresses in ABAQUS. The first one calculates the stresses more accurately by using "traction-separation" and Cohesive Zone Elements (CZE) [35]. The second method is simpler, by adding an extra layer of homogenous matrix material between every two plies of the composite. The layer can be as thin as $10 \mu m$, where the stresses in each layer can be inspected not to increase more than its mechanical strengths [36]. This method, although not entirely accurate, provides a preliminary estimation of whether the matrix will fail or not.

D. QUALITY CONTROL

1) CONSTITUENT CONTENT OF THE MATERIAL

Olson *et al.* [37] studied different types of defects in the compression strength and the inter-laminar shear strength of composites. They recommended a void content in the composite of less than 1% of the total volume, while Mallick [17] recommended a maximum void content of 2%. Olson *et al.* [37] also recommended the use of multi-stage curing for high thickness laminate to reduce fiber wrinkling during curing, which explains the results of experiments from 1986 done in US Navy Ship Research and Development Center, where they found that cylinders that were cured on Multi-stages survived higher pressures than the same ones that were cured in a single stage [13], [38]. Colombo and Vergani [31] recommended that the volume fraction of the fibers should be higher than 45% to improve the lamina strength in the transverse direction and avoid "Weepage" failure, which leaks fluids from the outside to the inside of the filament wound cylinder, or vice versa.

18 different samples were inspected and validated in order to assess the quality of the manufacturing. A tube was manufactured using filament winding, the intended manufacturing technique, and from the same fiber and matrix materials used in the design. 12 samples were tested using destructive methods and 6 were tested using non-destructive methods. The destructive method used in the analysis was acid digestion, while the non-destructive method was MicroCT scanning. The primary objective of the destructive method was to know
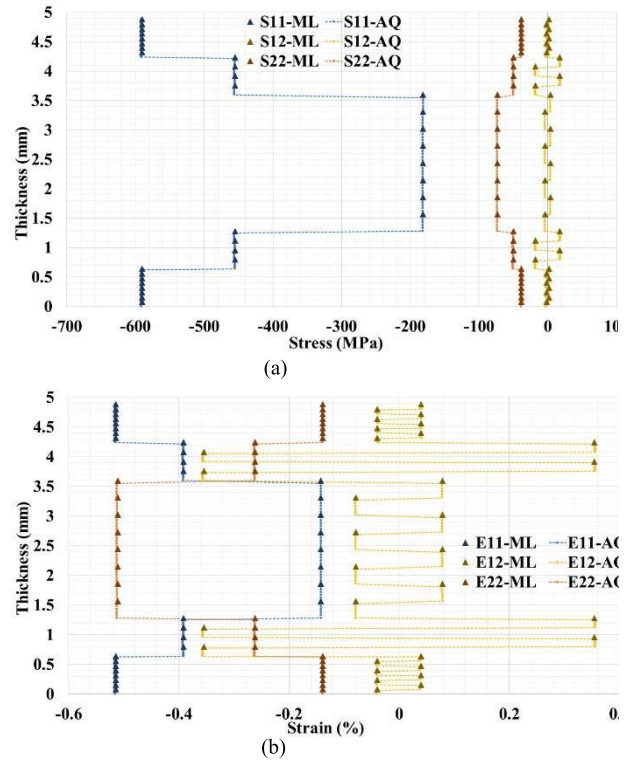
the fiber to matrix ratio, while the main aim of the non-destructive testing was to discover the accurate percentage of the voids in the material. Figure 8 shows some of the practical results of the two tests. A detailed description of the tests and the tests procedures has been reported in previous work [39].

The results of the void determination tests of the different samples indicated that the void content being less than 2%, the percentage recommended by Mallick [17]. The void content according to the non-destructive testing was 1.531%, and the Fiber/Matrix ratio according to the destructive one was 57.6 / 41.1 [39]. Judging by the results, the manufacturing facilities were deemed safe for the next phase, and the quality of the product will be in line with standards.

2) MOISTURE ABSORPTION

Carbon fiber reinforced epoxy (CFRE) composite, in general, has a drawback, especially in underwater and marine applications, which is moisture absorption. The word moisture does not mean necessarily water vapor but might also be used to describe the absorption of any vapor, condensate, or liquid that material is immersed in [40]. The water absorbed by the matrix forms a single hydrogen bond with the epoxy resin, breaking the Van der Waal bonds [41]. The absorbed water diffuses easily leading to the swelling of the material and inducing stresses in the laminate [42]. In addition to the swelling, the moisture absorbed by the resin decreases its
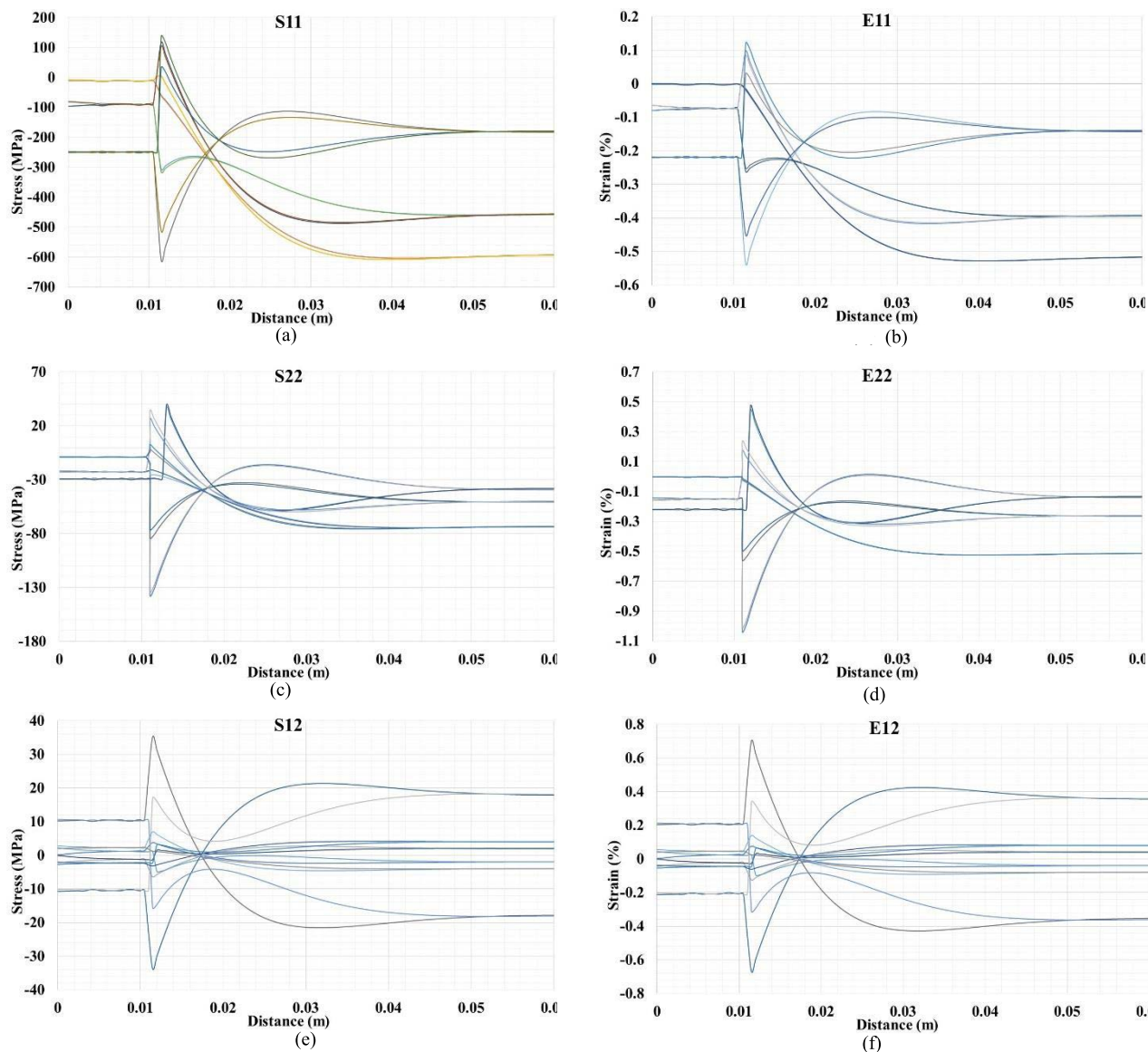
FIGURE 7. The stresses and strains across the length showing the effect of the endcap in; (a, b) the longitudinal direction, (c,d) the transverse direction, (e, f) the in-plane shear.
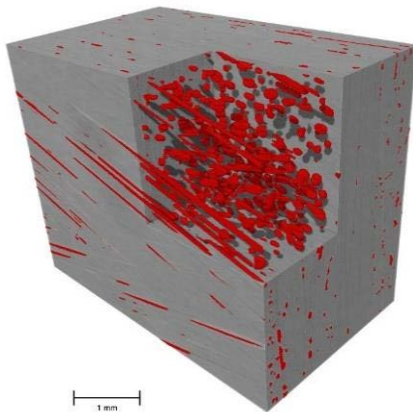
glass transition temperature, reducing the strength of the bond between the resin and the fibers. Much more importantly, since the aim of this work is to design the hull of an underwater vehicle, this amount of absorbed moisture, even if it is as low as 0.1% of the total weight, will affect the buoyancy of the vehicle. It is a well-known practice to design the underwater vehicles to be neutral in seawater, for ease of maneuvering, or slightly positive, in case of failure of one of the vehicle's components or loss of communication. The vehicle then surfaces preventing the loss of valuable assets. This buoyancy change, caused by the moisture absorption, might be considerable for the vehicle, depending on the diving period, size of the vehicle, and the thickness of the hull. For these reasons, the moisture absorption of the material had to be studied, especially at high depth. The hygral effect on CFRE, and the moisture saturation at different temperatures has been studied

in [43], [44], [45], and [46], but none of the previous literature, to the best of the author's knowledge, has studied the moisture saturation, at the targeted depth. Behera *et al.* [43] as well as Jesthi and Nayak [46] reported a reduction of 4% in the tensile strength after absorption saturation, while Li *et al.* [44] reported a 6% reduction. Behera *et al.*[43] also reported a 5% reduction in the compressive strength due to moisture absorption. Meng *et al.* [45], however, reported no noticeable change in the modulus of elasticity after moisture saturation in cross-plies laminate CFRP. All the percentage of change in the mechanical properties of the material, lie within the factor of safety included in the design. Hence, the main concern was moisture content increase, to be able to evaluate the buoyancy of the vehicle as noted previously.

Twelve filament wound samples, that were manufactured from the same materials used in the design, were immersed

FIGURE 9. Average value of the moisture absorption content of the twelve tested samples.

FIGURE 8. Example of the results of the micro voids tests; (a) fibers remaining after the itching process of the acid digestion tests, (b) reconstructed image resulting from the MicroCT scanning, showing the voids in red and the material in grey [39].

FIGURE 10. Hyperbaric pressure testing rig.

in seawater, taken from Oslo Fjord in Norway, in a pressure vessel at a high pressure to represent the immersion at the rated depth of the vehicle. The salinity of the seawater used in the tests was measured using a conductivity sensor and recorded to be 32.2 mS/cm. Six samples had a thickness of 2.25mm and the other six samples had a thickness of 3.25mm. The results of the tests are shown in Fig. 9. The through-the-surface moisture diffusivity factor was calculated to be $D_z|_{highdepth} = 72.7 \times 10^{-3} mm^2/day$. The testing procedures and calculations were performed as per the recommendations of standard [40].

These results are to be incorporated into the buoyancy calculations. Furthermore, a decision was made to coat the hull by using a thin external coating from another material, Nylon, or by using a thin layer of anti-fouling paint. This thin coating layer, exhibited in Fig. 1, although it might be moisture-absorbing itself by its nature, will reduce moisture absorption by the fibers and the matrix keeping the mechanical properties of the composite intact.

E. PRODUCTION

Two pilot samples were produced first, and each has a 250mm length with the same stacking sequence simulated. Since
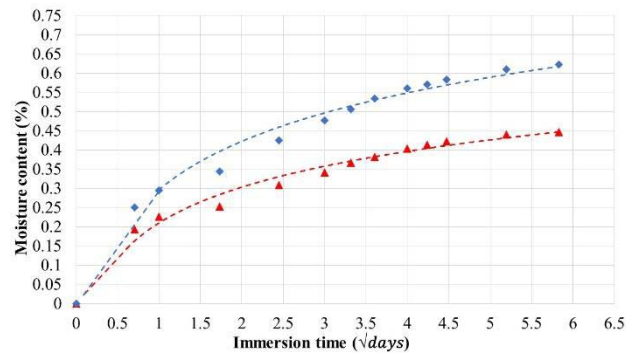
the stresses resulting from the endcap stabilize after 60mm, the length of the two pilot samples should be bigger than 120mm. Two endcaps were also designed and manufactured from aluminum and inserted into each side sealing the two ends using two sets of O-rings. The pressure vessel shown in Fig. 10 was used to test the samples.

One of the two samples was tested to the designated pressure, without taking the factor of safety into consideration, for 10 cycles, pressurizing with a rate of 45bar/min, maintaining the pressure for 1-4 hours, and depressurizing with the same rate, following the recommendations of standard [47]. A visual and detailed inspection of the sample was done first. Nevertheless, although the samples survived the testing cycles, a hidden failure, such as small delamination, could have occurred. This failure can increase with time and during the different cycles of use, resulting in a catastrophic failure and losing the vehicle permanently. Ultrasonic testing procedure was implemented to inspect the entire specimen for any hidden failures. This method is suitable for manual scanning of sub-surface imperfections, scanning the outside diameter of the composite, especially in small samples [48]. The device used, represented in Fig. 11, is GE Phasor XS,

FIGURE 11. GE Phasor XS and the probe used in the non-destructive testing.

FIGURE 12. Failure resulting from the implosion of the tube.

and the probe is 4MHz ($\pm$0.2MHz) angled at 45° ($\pm$1.5°). The results of the scan showed no clear damage.

The second pilot sample was fail tested till implosion, and it failed at approximately 93% of the predicted failure pressure. The failure was discovered mainly after the endcap region as predicted earlier, as shown in Fig. 12. It should be also noted that such an experiment is not always favorable since the resulting pressure wave from the implosion, might damage or even fail the testing equipment, but this experiment was needed in this specific case, to ensure that the material properties obtained from the characterization phase are correct, fairly.

III. DISCUSSION AND CONCLUSION

This paper tackles the design of the hull of a small autonomous underwater vehicle rated at 2000m depth. It provided a detailed description of every step of the design process. Composites were used in the design, in particular CFRE, given their higher strength-to-weight ratio than metals, which in return will produce a lighter hull with a thinner thickness. A selection was made between two manufacturing methods, sheet wrapping, and filament winding. The filament winding process was used since the technique is more automated than sheet wrapping and more appropriate for mass production.

Due to the missing values of the properties of the composite, whether in the material datasheet or in previous literature, a material characterization was performed by testing the composite under compression loading in longitudinal and transverse directions. Tubes were wounded in different orientations to assess different properties, and each tube was cut longitudinally into four pieces, each piece was tested as a sample. The testing standard used was ASTM-D6641 and special fixtures were manufactured to grip the curved samples. The procedure proved effective in all the winding angles tested, except in the longitudinal winding where two samples failed outside the gauge section.

Two models were created for simulating the stresses and the material behavior under loading. One is an analytical model using MATLAB and the other is an FE model using ABAQUS software. The analytical model was also employed in optimizing the plies' angles, sequence, and number. The FEM was used however to simulate the effect of the endcaps plugging and sealing the hull from both sides, which induces further stresses that cannot be simulated using the analytical model. The results of both models were compared to each other in furtherance of validation.

Afterwards, pilot samples were manufactured and tested for microporosity, using acid digestion and MicroCT scanning, as well as moisture absorption of seawater under high pressure. The voids content did not increase over 2%, as recommended by Mallick [17]. The material characteristics after the seawater absorption were still within the safety margin used during the design. The moisture content of the material was integrated into the buoyancy calculations of the vehicle.

Finally, two samples were manufactured using the stacking sequence designed, plugged using aluminum endcaps sealed with O-rings, and tested in a hyperbaric testing chamber several times. The samples were visually inspected first and then inspected using ultrasonic non-destructive testing for any hidden failures. After the samples had passed the inspection, the decision was taken to move forward safely with the production phase.

The pressure hull was manufactured with the designed length coated for moisture absorption, and painted for high visibility in seawater, as shown in Fig. 1.

REFERENCES

[1] D. L. Rudnick, R. E. Davis, C. C. Eriksen, D. M. Fratantoni, and M. J. Perry, "Underwater gliders for ocean research," *Mar. Technol. Soc. J.*, vol. 38, no. 2, pp. 73–84, 2004.

[2] W. P. Barker, "An analysis of undersea glider architectures and an assessment of undersea glider integration into undersea applications," Dept. Syst. Eng., Naval Postgraduate School, Monterey, CA, USA, Tech. Rep., 2012. [Online]. Available: https://apps.dtic.mil/sti/citations/ADA567412

[3] R. E. Davis, C. C. Eriksen, and C. P. Jones, "Autonomous buoyancy-driven underwater gliders," in *The Technology and Applications of Autonomous Underwater Vehicles*. 2002, pp. 37–58.

[4] D. Fenucci, A. Munafo, A. B. Phillips, J. Neasham, N. Gold, J. Sitbon, I. Vincent, and T. Sloane, "Development of smart networks for navigation in dynamic underwater environments," in *Proc. IEEE/OES Auto. Underwater Vehicle Workshop (AUV)*, Nov. 2018, pp. 1–6, doi: 10.1109/AUV.2018.8729779.

[5] A. B. Phillips, N. Gold, N. Linton, C. A. Harris, E. Richards, R. Templeton, S. Thune, J. Sitbon, M. Müller, I. Vincent, and T. Sloane, "Agile design of low-cost autonomous underwater vehicles," in *Proc. OCEANS-Aberdeen*, Jun. 2017, pp. 1–7, doi: 10.1109/OCEANSE.2017.8084772.

[6] P. E. Hagen, N. Storkersen, K. Vestgard, and P. Kartvedt, "The HUGIN 1000 autonomous underwater vehicle for military applications," in *Proc. Oceans Celebrating Past... Teaming Toward Future*, vol. 2, Sep. 2003, pp. 1141–1145, doi: 10.1109/OCEANS.2003.178504.

[7] K. Maritime. *Autonomous Underwater Vehicle—AUV The HUGIN Family*. Accessed: Jul. 2022. [Online]. Available: https://www.kongsberg.com/globalassets/maritime/km-products/product-documents/hugin-family-of-auvs

[8] C. C. Eriksen, "Seaglider: A long-range autonomous underwater vehicle for oceanographic research," *IEEE J. Ocean. Eng.*, vol. 26, no. 4, pp. 424–436, Oct. 2001, doi: 10.1109/48.972073.

[9] S. Wood and A. Inzartsev, "Autonomous underwater gliders," in *Underwater Vehicles*. 2009, pp. 499–524, doi: 10.5772/6718.

[10] E. G. Anderlini Thomas, S. C. Woodward, D. A. Real-Arce, T. Morales, C. Barrera, and J. J. Hernández-Brito, "Identification of the dynamics of biofouled underwater gliders," in *Proc. IEEE/OES Auton. Underwater Vehicles Symp. (AUV)*, Sep. 2020, pp. 1–6, doi: 10.1109/AUV50043.2020.9267919.

[11] C. Yu, Q. Guo, X. Gong, Y. Yang, and J. Zhang, "Fatigue life assessment of pressure hull of deep-sea submergence vehicle," *Ocean Eng.*, vol. 245, Feb. 2022, Art. no. 110528, doi: 10.1016/j.oceaneng.2022.110528.

[12] A. B. Strong, *Fundamentals of Composites Manufacturing: Materials, Methods and Applications*. Southfield, MI, USA: Society of Manufacturing Engineers, 2008.

[13] T. J. Osse and T. J. Lee, "Composite pressure hulls for autonomous underwater vehicles," in *Proc. OCEANS*, Sep. 2007, pp. 1–14, doi: 10.1109/OCEANS.2007.4449124.

[14] H. Garala, "Structural evaluation of 8-inch diameter graphite-epoxy composite cylinders subjected to external hydrostatic compressive loading," David Taylor, Bethesda, MD, USA, Res. Center Rep. DTRC-89/016, 1989.

[15] O.-I. Byon, J. Vinson, and S. Sato, "Analysis of various thick-walled cross-ply composite cylindrical shells subjected to lateral pressures," *Compos. B, Eng.*, vol. 27, no. 6, pp. 651–655, 1996, doi: 10.1016/1359-8368(95)00049-6.

[16] S. T. Peters, *Composite Filament Winding*. ASM International, USA, 2011. [Online]. Available: https://www.asminternational.org/

[17] P. K. Mallick, *Fiber-Reinforced Composites: Materials, Manufacturing, and Design*. Boca Raton, FL, USA: CRC Press, 2007.

[18] D. Gay and S. V. Hoa, *Composite Materials: Design and Applications*. Boca Raton, FL, USA: CRC Press, 2007.

[19] *Compressive Properties of Polymer Matrix Composite Materials With Unsupported Gage Section by Shear Loading*, D. ASTM, Standard D3410-03, 2016.

[20] *Standard Test Method for Compressive Properties of Polymer Matrix Composite Materials Using a Combined Loading Compression (CLC) Test Fixture*, D. ASTM, Standard D6641, 2016.

[21] *Standard Test Method for Tensile Properties of Polymer Matrix Composite Materials*, D. ASTM, Standard ASTM D3039, 2017.

[22] T. C. Henry, C. E. Bakis, and E. C. Smith, "Determination of effective ply-level properties of filament wound composite tubes loaded in compression," *J. Test. Eval.*, vol. 43, no. 1, pp. 96–107, 2015, doi: 10.1520/JTE20130159.

[23] A. R. Bunsell, *Handbook of Properties of Textile and Technical Fibres*. Sawston, U.K.: Woodhead Publishing, 2018.

[24] N. Oya and D. J. Johnson, "Longitudinal compressive behaviour and microstructure of PAN-based carbon fibres," *Carbon*, vol. 39, no. 5, pp. 635–645, 2001, doi: 10.1016/S0008-6223(00)00147-0.

[25] D. F. Adams and J. S. Welsh, "The Wyoming combined loading compression (CLC) test method," *J. Compos., Technol. Res.*, vol. 19, no. 3, pp. 123–133, 1997, doi: 10.1520/CTR10023J.

[26] B. W. Rosen, "A simple procedure for experimental determination of the longitudinal shear modulus of unidirectional composites," *J. Compos. Mater.*, vol. 6, no. 3, pp. 552–554, Jul. 1972, doi: 10.1177/002199837200600310.

[27] *Standard Test Methods for Density and Specific Gravity (Relative Density) of Plastics by Displacement*, D. ASTM, Standard D792, 2008.

[28] T. Messager, M. Pyrz, B. Gineste, and P. Chauchot, "Optimal laminations of thin underwater composite cylindrical vessels," *Compos. Struct.*, vol. 58, no. 4, pp. 529–537, 2002, doi: 10.1016/S0263-8223(02)00162-9.

[29] M. Reza Khoshravan Azar, A. A. Emami Satellou, M. Shishesaz, and B. Salavati, "Calculating the optimum angle of filament-wound pipes in natural gas transmission pipelines using approximation methods," *J. Pressure Vessel Technol.*, vol. 135, no. 2, Apr. 2013, doi: 10.1115/1.4007189.

[30] P. Geng, J. Z. Xing, and X. X. Chen, "Winding angle optimization of filament-wound cylindrical vessel under internal pressure," *Arch. Appl. Mech.*, vol. 87, no. 3, pp. 365–384, Mar. 2017, doi: 10.1007/s00419-016-1198-5.

[31] C. Colombo and L. Vergani, "Optimization of filament winding parameters for the design of a composite pipe," *Compos. B, Eng.*, vol. 148, pp. 207–216, Sep. 2018, doi: 10.1016/j.compositesb.2018.04.056.

[32] A. F. Hamed, Y. A. Khalid, S. M. Sapuan, M. M. Hamdan, T. S. Younis, and B. B. Sahari, "Effects of winding angles on the strength of filament wound composite tubes subjected to different loading modes," *Polym. Polym. Compos.*, vol. 15, no. 3, pp. 199–206, Mar. 2007, doi: 10.1177/096739110701500304.

[33] J. H. S. Almeida, M. L. Ribeiro, V. Tita, and S. C. Amico, "Stacking sequence optimization in composite tubes under internal pressure based on genetic algorithm accounting for progressive damage," *Compos. Struct.*, vol. 178, pp. 20–26, Oct. 2017, doi: 10.1016/j.compstruct.2017.07.054.

[34] *ABAQUS*, Dassault Systèmes, Vélizy-Villacoublay, France, 2020.

[35] E. J. Barbero, *Finite Element Analysis of Composite Materials Using Abaqus*. Boca Raton, FL, USA: CRC Press, 2013.

[36] H. Dodiuk, *Handbook of Thermoset Plastics*, 3rd ed. 2014.

[37] B. Olson, M. Lamontia, J. Gillespie, and T. Bogetti, "Effects of defects on compression and interlaminar shear performance of thermoplastic composites," Dupont Adv. Mater. Syst., Newark, DE, USA, Tech. Rep., 1994.

[38] H. J. Garala, "Structural evaluation of externally pressurized graphite-composite cylinders," David Taylor Naval Ship Res. Develop. Center, MD, USA, Tech. Rep., 1986.

[39] M. Elkolali, L. P. Nogueira, P. O. Rønning, and A. Alcocer, "Void content determination of carbon fiber reinforced polymers: A comparison between destructive and non-destructive methods," *Polymers*, vol. 14, no. 6, p. 1212, Mar. 2022, doi: 10.3390/polym14061212.

[40] D. Astm, *Standard Test Method for Moisture Absorption Properties and Equilibrium Conditioning of Polymer Matrix Composite Materials*, ASTM International, West Conshohocken, PA, USA, Standard 5229/D5229M-14e1, 2014, doi: 10.1520/D5229_D5229M-20.

[41] J. Zhou and J. P. Lucas, "Hygrothermal effects of epoxy resin. Part I: The nature of water in epoxy," *Polymer*, vol. 40, no. 20, pp. 5505–5512, 1999, doi: 10.1016/S0032-3861(98)00790-3.

[42] E. Pérez-Pacheco, J. I. Cauich-Cupul, A. Valadez-González, and P. J. Herrera-Franco, "Effect of moisture absorption on the mechanical behavior of carbon fiber/epoxy matrix composites," *J. Mater. Sci.*, vol. 48, no. 5, pp. 1873–1882, Mar. 2013, doi: 10.1007/s10853-012-6947-4.

[43] A. Behera, A. Vishwakarma, M. M. Thawre, and A. Ballal, "Effect of hygrothermal aging on static behavior of quasi-isotropic CFRP composite laminate," *Compos. Commun.*, vol. 17, pp. 51–55, Feb. 2020, doi: 10.1016/j.coco.2019.11.009.

[44] H. Li, K. Zhang, X. Fan, H. Cheng, G. Xu, and H. Suo, "Effect of seawater ageing with different temperatures and concentrations on static/dynamic mechanical properties of carbon fiber reinforced polymer composites," *Compos. B, Eng.*, vol. 173, Sep. 2019, Art. no. 106910, doi: 10.1016/j.compositesb.2019.106910.

[45] M. Meng, M. J. Rizvi, S. M. Grove, and H. R. Le, "Effects of hygrothermal stress on the failure of CFRP composites," *Compos. Struct.*, vol. 133, pp. 1024–1035, Dec. 2015, doi: 10.1016/j.compstruct.2015.08.016.

[46] D. K. Jesthi and R. K. Nayak, "Evaluation of mechanical properties and morphology of seawater aged carbon and glass fiber reinforced polymer hybrid composites," *Compos. Part B: Eng.*, vol. 174, Oct. 2019, Art. no. 106980, doi: 10.1016/j.compositesb.2019.106980.

[47] *Rules for Building and Classing: Underwater Vehicles, Systems and Hyperbaric Facilities*, Amer. Bur. Shipping (ABS), Houston, TX, USA, 2012.

[48] *Standard Guide for Nondestructive Examination of Composite Overwraps in Filament Wound Pressure Vessels Used in Aerospace Applications*, E. ASTM, Standard E2981-21, 2021.

• • •